Rolinski, Susanne et al.

Article — Published Version

Dynamics of soil organic carbon in the steppes of Russia and Kazakhstan under past and future climate and land use

Regional Environmental Change

Provided in Cooperation with:
Leibniz Institute of Agricultural Development in Transition Economies (IAMO), Halle (Saale)

Suggested Citation: Rolinski, Susanne et al. (2021) : Dynamics of soil organic carbon in the steppes of Russia and Kazakhstan under past and future climate and land use, Regional Environmental Change, ISSN 1436-378X, Springer, Berlin, Vol. 21, Iss. 3, https://doi.org/10.1007/s10113-021-01799-7

A Composition of the natural vegetation

Table S1: Representatives of the plants in the natural vegetation (PFTs) in the VLC region and the corresponding species.

name	description	species
TeBS	temperate broadleaved summergreen deciduous trees	oak or beech trees
BoNE	boreal needleleaved evergreen trees	fir or spruce trees
BoBS	boreal broadleaved summergreen trees	birch trees
C3G	C3 grasses	vegetation with C3 grasses

LPJmL simulates plausible spatial vegetation patterns of sparsely vegetated areas and steppes. This also holds for the VLC region for which the model reproduced the gradient of the steppe vegetation without trees in the southwest to woody steppe and forest vegetation in the northeast (Fig. S1). The simulated vegetation at 1990 was dominated by trees in the northeast (Fig. S1a) and by herbaceous vegetation in the southwest (Fig. S1b).

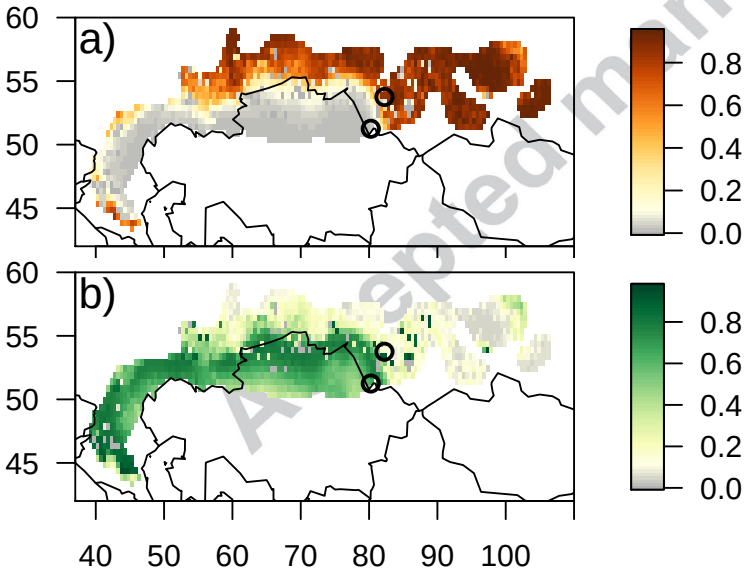

Fig. S1: Fraction of the canopy cover of the natural vegetation types (FPC $\in$ [0,1]) for a 10 year average around 1990 for tree (a) and herbaceous (b) vegetation. Axes denote longitude and latitude and lines country borders. Circles denote positions L1 and L2 of Fig. S3.

The subregions are covered with different vegetation types (Tab. S2): sparse and grassland dominated in R1, denser with more trees than grasses in R2, closed and forested in R3 and sparsely with more trees than grasses in R4.

Table S2: Vegetation composition in the subregions of the VLC area

Region	Total coverage	Trees	Grasses
1	78±22%	13±18%	65±21%
2	95±18%	72±21%	23±15%
3	100±0.2%	87±12%	13±12%
4	79±23%	30±33%	49±26%

The future distribution of vegetation types is expected to change as the treeline recedes towards the north under warming. For the A2 scenario and the GCM UKMO HadCM3, tree vegetation at the end of the 21^{st} century declines in the VLC region northeast of Kazakhstan while herbaceous vegetation (Fig. S2b) became more dominant (Fig. S2a). The location where the vegetation type changed from herbaceous to trees (treeline) was simulated for 1990 at, e.g., 55.10° N or 52.92° N (at longitudes 78.25° E and 59.25° E, respectively). For 2090, the treeline at these longitudes occurred further north at 55.85° N or 53.90° N, respectively, equivalent to a shift of between 83 and 104 km within 100 years. In the Russian VLC area northwest of Kazakhstan, herbaceous vegetation was replaced by trees (blueish colours in Fig. S2a). In the western part, herbaceous vegetation slightly increased.

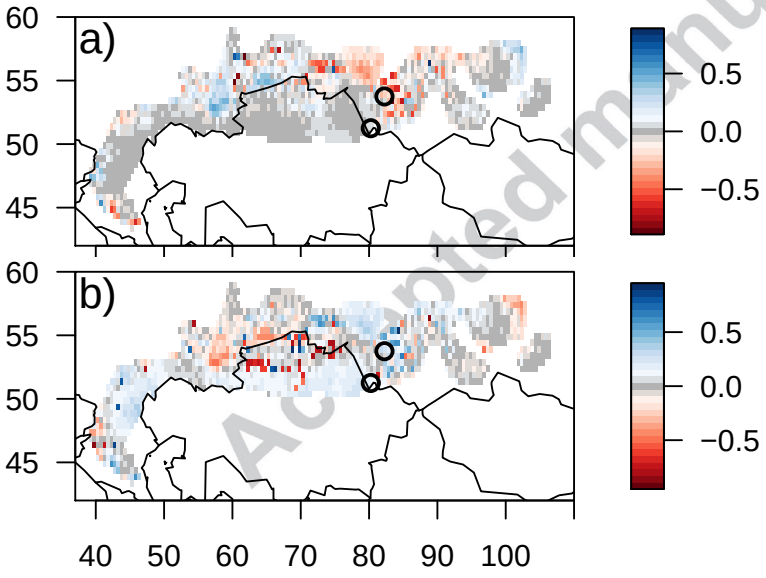

Fig. S2: Difference maps of the fraction of the canopy cover of the natural vegetation types (FPC ∈ [0,1]) for a 10-year average around 2090 and 1990 for tree (a) and herbaceous (b) vegetation (simulation with GCM UKMO HadCM3 and the A2 scenario). Axes denote longitude and latitude and lines country borders. Circles denote positions L1 and L2 of Fig. S3.

The shift of the treeline reflects changes in the vegetation composition, only influenced by changing climatic conditions (Fig. S3). The vegetation in the northeast (e.g. at L1, Fig. S3 left, northern dot in Fig. S1) was composed in the 1950's mainly of boreal evergreen

coniferous (BoNE) and boreal summergreen deciduous (BoBS) trees, with a fluctuating proportion of C3-grasses (C3G) (Tab. S1 for vegetation type description). This composition was replaced in the middle of the 21^{st} century by C3G before temperate summergreen deciduous trees (TeBS) begin to establish at the end of the 21^{st} century and cover about 20% of the area. The degree of the replacement of trees by grasses differed for the climate scenarios with highest herbaceous vegetation cover for A2 and lowest for B1. In the southern part (e.g. at L2, Fig. S3 right, southern dot in Fig. S1), the herbaceous vegetation dominated throughout the 21^{st} century. Only minor area proportions were covered by trees (BoBS and TeBS).

The contribution of the PFTs to the vegetation composition in the 1990s (Fig. S1) in the subregions described above can be summarized as: a) dry steppe in region R1 with predominant C3G coverage (71.5±30.5%) and small contributions of trees (BoBS 5.1%, TeBS 5.6% and BoNE 2.7%); b) in region R2 in the north, where BoBS trees had an average coverage of 46±29%, BoNE about 24±26% and grasses about 21±23%; c) forest steppe in R3 with mostly trees (BoNE 52±23% and BoBS of 28±17%) and grass coverage of 19±15% and sparse vegetation in R4 with partly trees (30±34%) and grasses (49±26%).

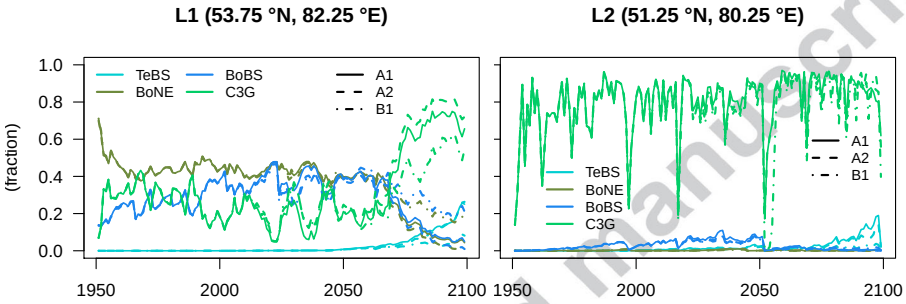

Fig. S3: Fraction of plant functional types from 1951 to 2100 for two locations: L1 in the forested area (left) and L2 the grassland steppe region (right). Results are shown for the GCM UKMO HadCM3 and all SRES scenarios.

Differences in the vegetation composition are also reflected by regional differences in evapotranspiration (ET). Simulated annual average evapotranspiration from 1900 to 2020 was 265 ± 20 mm a^{-1} (Fig. S10). Depending on the SRES climate scenarios, evapotranspiration increased until 2100 with an annual rate of 0.68 (A1), 0.58 (A2) and 0.39 (B1) mm a^{-1}, calculated using the Mann-Kendall trend test. Average evapotranspiration before 2020 ranged from 239 ± 24 mm a^{-1} in the eastern R1 to 310 ± 42 mm a^{-1} in the western R3 (Fig. S10 lower left). The increasing trends after 2020 are lowest for the scenario B1 in the eastern R3 (0.29) and highest in the western R1 (0.48). In the emission scenario A2 with higher temperatures, the trends are higher (from 0.31 in R1 to 0.86 in the northern R2).

B Description of SRES scenario details

The scenarios for climate projections until the year 2100 were based on the storylines of the IPCC Special Report on Emissions Scenarios (SRES, Nakićenović et al, 2000). From the four storylines (A1, A2, B1, B2) which were based on diverging assumptions on the societal development concerning economic growth as well as regional connectivity, we describe here the marker scenarios for the A1, A2 and B1 scenario families.

Scenario A1 describes a world emphasizing economic growth with converging regional average income per capita which resulted from technological advances and international cooperation. In the A1B marker scenario, which was based on fossil as well as non-fossil energy sources, future GHG emissions steeply increased in the first decades of the 21^{st} century and stabilized until the end of the century at an atmospheric CO_2 concentration of 700 ppm.

In the A2 scenario, economic growth is realized in a segregated world with slower technological change and differentiation into economic regions. Since heterogeneous technology and resource distributions prevailed, final energy intensities in A2 declined, so that GHG emissions increased throughout the century and reached a CO_2 concentration of 820 ppm.

In contrast, the B1 scenario describes a world developing towards a sustainable economy with societies having a stronger environmental awareness even without implementing any climate policies. GHG emissions were below those of A1 since post-fossil technologies were implemented mostly, driven by environmental concerns, so that the CO_2 concentration remained below 550 ppm.

C Historical land-change reconstruction for the VLC region

Land-use data in the VLC area and the former Soviet Union from 1940 to 2012 was reconstructed based on the detailed official reports by the Soviet Union and later by Kazakhstan and Russia at the province (oblast level, Tab. S3) on sown areas for major crop types, namely, total sown area, sown grain crops, sugar beets, sunflower, potatoes, vegetables. as well as yields.

In total, 14 contemporary provincial units were covered in Kazakhstan and 71 in Russia. From 1940 to 2012 there have been data gaps, for instance, from 1975 to 1979 and from 1981 to 1984 which were interpolated based on the overall trajectory of cropland dynamic across the Kazakhstan and Russia and proportions of cropland acreage of each province (oblast). We also had to combine certain administrative units in Kazakhstan and Russia, due to a change of administrative boundaries particularly before 1950 and after 1990. The new dataset better reflected cropland expansion and abandonment compared to HYDE, which is based on cropland dynamics and population counts, but not on sown areas for the former Soviet Union.

To reconstruct the location of the VLC area we also utilized the archival maps of the Campaign and spatial-allocation modeling (Schierhorn et al, 2013; Meyfroidt et al, 2016). To reconstruct cropland dynamics from 1940 to 2012, we first developed a cropland mask for 2009 based on reclassified land-cover map for Kazakhstan (circa 2009, thematic class (Klein et al, 2012) and land-cover map for Russia (Bartalev et al, 2016). We then spatially allocated sown-area statistics and calculated proportions of crops at province level following Schierhorn et al (2013) and traced cropland expansion and cropland contraction (abandonment) back to 1940. We developed rules for spatial allocation of sown area for the entire VLC area with the use of 1:3,000,000 archival map of the VLC cropland expansion in Kazakhstan from 1954 until the peak of the VLC in 1961 from the Atlas of the Virgin Territory (Atlas Celinnogo Kraja) (Moscow State University, 1964).

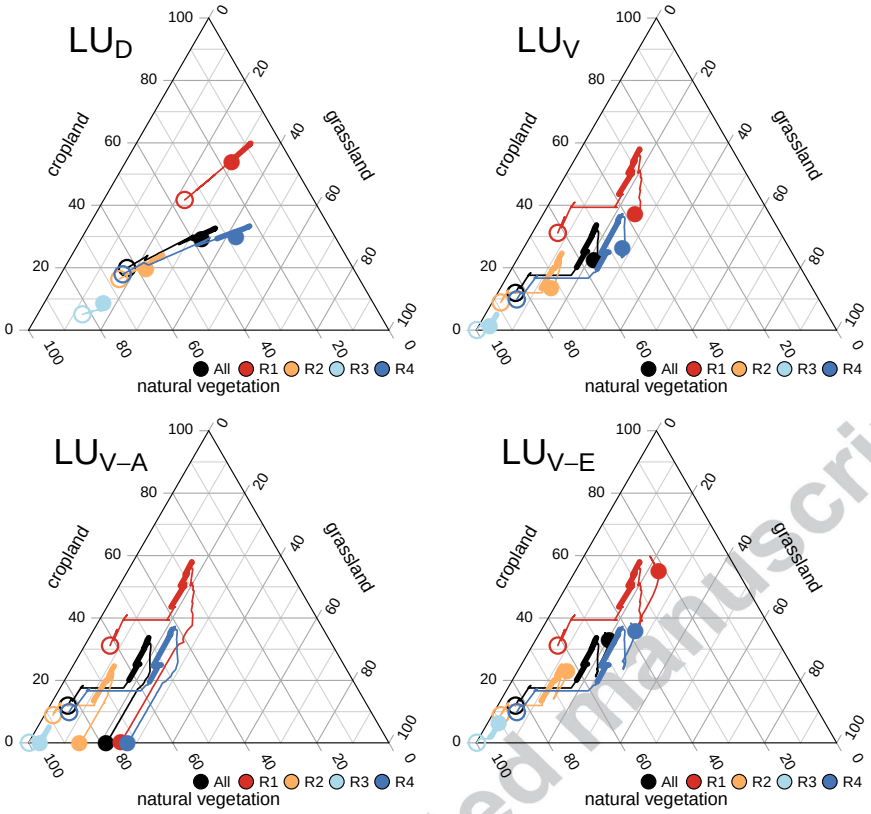

Fig. S4: Land-use characteristics from 1900 to 2100 for the four datasets in percentages of cropland, grassland and natural vegetation. Subregions are color-coded and symbols used to denote the begin of the timeseries in 1900 (open circle) and the end in 2100 (filled circle). The increased line thickness is chosen for the VLC era from 1954 to 1963.

Table S3: Sources of sown areas for major crops at province (oblast) level.

Russia
USSR SSPH (1957) National Economy of RSFSR in 1956. Statistical yearbook. Moscow: State Statistical Publishing House.
USSR SSPH (1959) National Economy of RSFSR in 1958. Statistical yearbook. Moscow: State Statistical Publishing House.
USSR CSD (1960) National Economy of RSFSR in 1959. Statistical yearbook. Moscow: Gosstatizdat, Central Statistical Department.
USSR CSD (1961) National Economy of RSFSR in 1960. Statistical yearbook. Moscow: Gosstatizdat, Central Statistical Department.
USSR CSD (1962) National Economy of RSFSR in 1961. Statistical yearbook. Moscow: Gosstatizdat, Central Statistical Department.
USSR CSD (1963) National Economy of RSFSR in 1962. Statistical yearbook. Moscow: Gosstatizdat, Central Statistical Department.
USSR CSD (1965) National Economy of RSFSR in 1964. Statistical yearbook. Moscow: Statistika, Central Statistical Department.
USSR CSD (1968) National Economy of RSFSR in 1967. Statistical yearbook. Moscow: Statistika, Central Statistical Department.
USSR CSD (1971) National Economy of RSFSR in 1969. Statistical yearbook. Moscow: Statistika, Central Statistical Department.
USSR CSD (1973) National Economy of RSFSR in 1972. Statistical yearbook. Moscow: Statistika, Central Statistical Department.
USSR CSD (1974) National Economy of RSFSR in 1973. Statistical yearbook. Moscow: Statistika, Central Statistical Department.
USSR CSD (1976) National Economy of RSFSR in 1975. Statistical yearbook. Moscow: Statistika, Central Statistical Department.
USSR CSD (1978) National Economy of RSFSR in 1977. Statistical yearbook. Moscow: Statistika, Central Statistical Department.
USSR CSD (1981) National Economy of RSFSR in 1980. Statistical yearbook. Moscow: Finansi i Statistika, Central Statistical Department.
USSR CSD (1983) National Economy of RSFSR in 1982. Statistical yearbook. Moscow: Finansi i Statistika, Central Statistical Department.
USSR CSD (1984) National Economy of RSFSR in 1983. Statistical yearbook. Moscow: Finansi i Statistika, Central Statistical Department.
USSR CSD (1986) National Economy of RSFSR in 1985. Statistical yearbook. Moscow: Finansi i Statistika, Central Statistical Department.
USSR CSD (1987) National Economy of RSFSR in 1986. Statistical yearbook. Moscow: Finansi i Statistika, Central Statistical Department.
USSR CSD (1988) National Economy of RSFSR in 1987. Statistical yearbook. Moscow: Information-Publishing Center, Central Statistical Department.
USSR CSD (1990) National Economy of RSFSR in 1989. Statistical yearbook. Moscow: Republican Information-Publishing Center, Central Statistical Department.
Kazakhstan
KAZSTAT. (2000) Agriculture, Forestry and Fishing in Kazakhstan in 1999. Statistical Yearbook. Almaty: Agency of Statistics of Kazakhstan.
KAZSTAT. (2001) Industry, Agriculture and Construction in Kazakhstan for 1920-2000. Statistical Compendium. Almaty: Agency of Statistics of Kazakhstan.
KAZSTAT. (2005) Agriculture, Forestry and Fishing in Kazakhstan in 2000-. Statistical Yearbook. Almaty: Agency of Statistics of Kazakhstan.
KAZSTAT. (2009) Agriculture, Forestry and Fishing in Kazakhstan in 2004-. Statistical Yearbook. Almaty: Agency of Statistics of Kazakhstan.
KAZSTAT. (2011) Agriculture, Forestry and Fishing in Kazakhstan in 2006. Statistical Yearbook. Almaty: Agency of Statistics of Kazakhstan.
KAZSTAT. (2003) Republic of Kazakhstan: 50 years since the beginning of the Virgin Lands Campaign. Statistical yearbook. Almaty: Agency of Statistics of Kazakhstan.

D Comparison with SOC data

Table S4: Regional coverage and sources of SOC data used for comparison with model results

Region	Source
Altai Krai	Bischoff et al (2016)
Rostov Oblast	Ovsepyan et al (2019, 2000)
Novosibirsk Oblast	Smolentseva et al (2018)
Buryat Republic	Chimitdorzhieva (2017); Lavrentyeva et al (2017)
Orenburg Oblast	Sablina (2015)
Khakass Republic	Kutkina and Eremina (2011, 2013)
Uralsk Oblast	Baranova and Rakhimgalieva (2008)

For the comparison of simulation results to observed data, these were aggregated to the depth layers of the model LPJmL: 0-20, 20-50, 50-100, 100-200 and 200-300 cm (Tab. S4). SOC simulation results per soil layer were aggregated as cumulative sums until the respective depth of the layer. Observations are included as colored dots in maps (Fig. S5) and in scatter plots (Fig. S6). The scatter plots show each of the values for the same location which are overlayn in the maps. Details of the regressions per soil layer are given in Tab. S5.

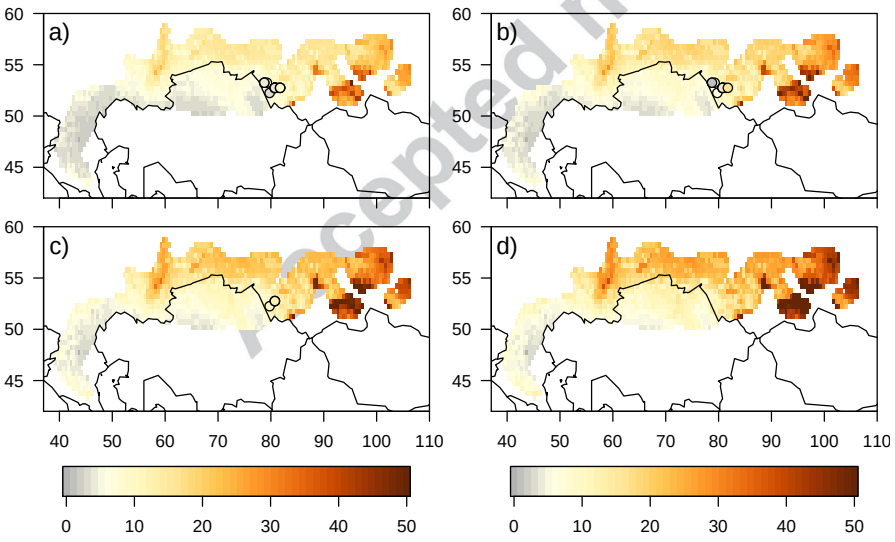

Fig. S5: Soil organic carbon content (gC m^{-2}) of simulations with LPJmL and measured values (see Tab. S4) per soil layer depths. Panels combine measurements (colored dots) and map of simulated values cumulated per soil layer. Shown are layer 2 (a) to 5 (d).

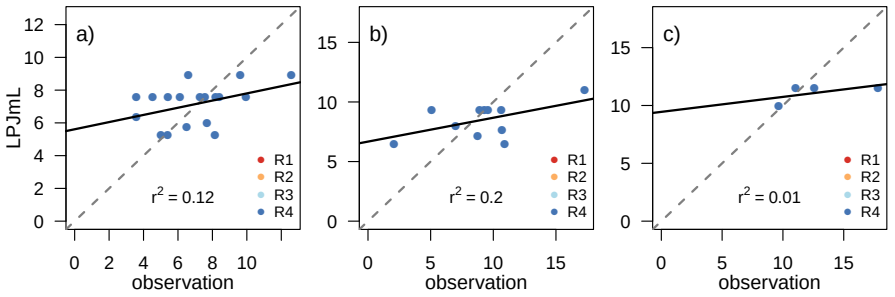

Fig. S6: Soil organic carbon content of simulations with LPJmL and measured values (see Tab. S4). Panels show cumulative values from layers 2 (a) to 4 (c) with the regression line (solid line). Colors indicate the southern central subregion (R4) in which the observations were made.

Table S5: Regression details for the comparison of SOC simulation results and observations in the soil layers (cm) in VLC region.

Layer	From	To	Intercept	slope	r	p-value	N
1	0	20	0.59	0.84	0.54	< 0.001	34
2	0	50	5.48	0.41	0.46	< 0.001	26
3	0	100	6.67	0.20	0.20	0.09	11
4	0	200	9.45	0.13	0.01	0.42	4

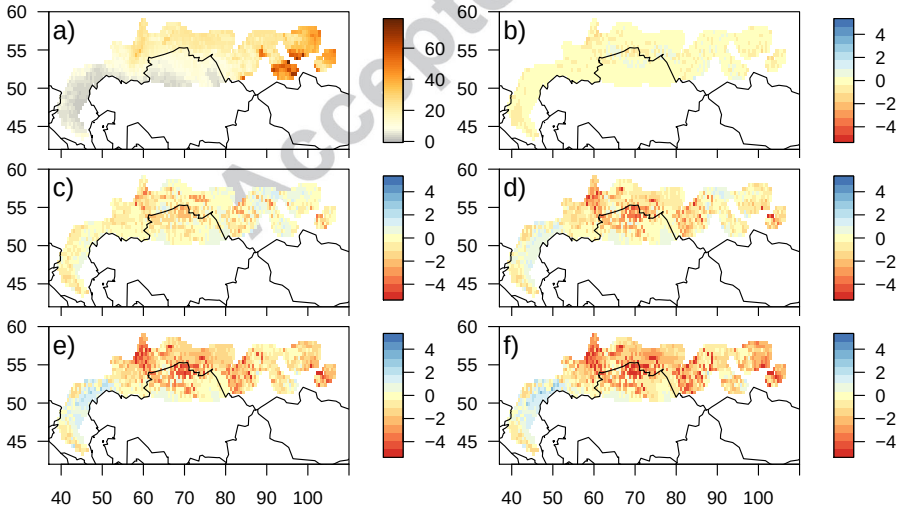

Fig. S7: Soil organic carbon stock (kgC m^{-2}) in the VLC region when applying land-use data set LU_V in absolute values (average over 1925 to 1940) (a) and differences to this period for the five following time periods (b to f, see Tab. 2).

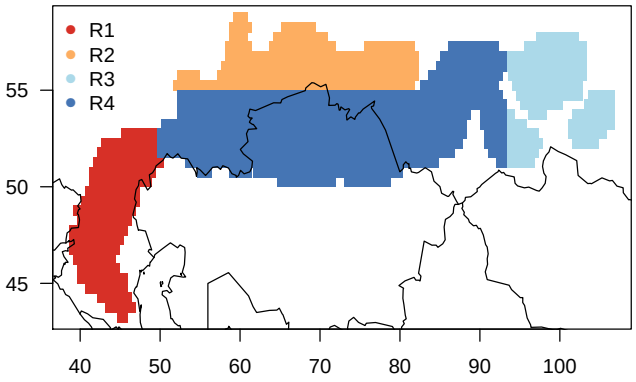

Fig. S8: Map of VLC region with location of subregions for detailed analysis.

E Definition of subregions of VLC area

We defined four subregions with different landuse histories and climatic conditions for a detailed analysis of the carbon stocks and fluxes, description see section 2.7.

Region R1 in the south-western part (west of 50° W and south of 55° N) is characterized by dry steppe and moderate temperatures (Fig. S9). In the northern part (north of 55° N and west of 82° E), region R2, forest is dominant and recieves precipitation between 450 and 550 mm a^{-1}. Region R3 in the eastern part (east of 93° E) is mostly covered by forest and is characterized by higher precipitation and lower temperatures. The central southern region R4 receives the lowest precipitation (380 to 450 mm a^{-1}) and was the most intensely used area with 80 Mha cropland, included 80% of the cropland expansion during the VLC.

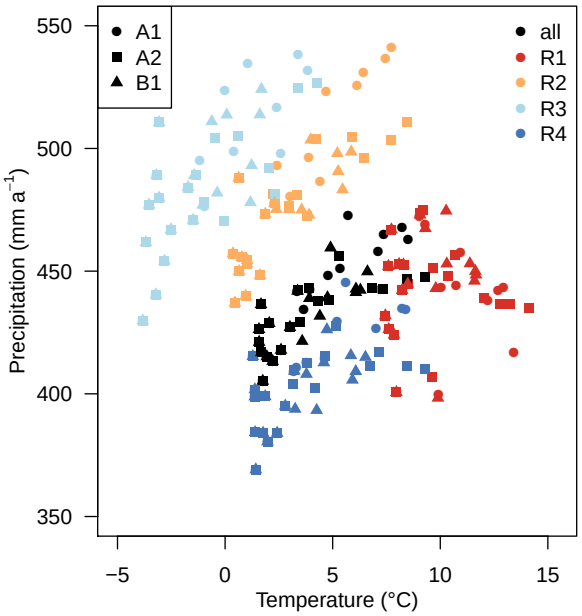

Fig. S9: Average temperature and precipitation values per region (colors), SRES scenario (symbols) and decade from 1900 to 2100.

F Average regional timeseries

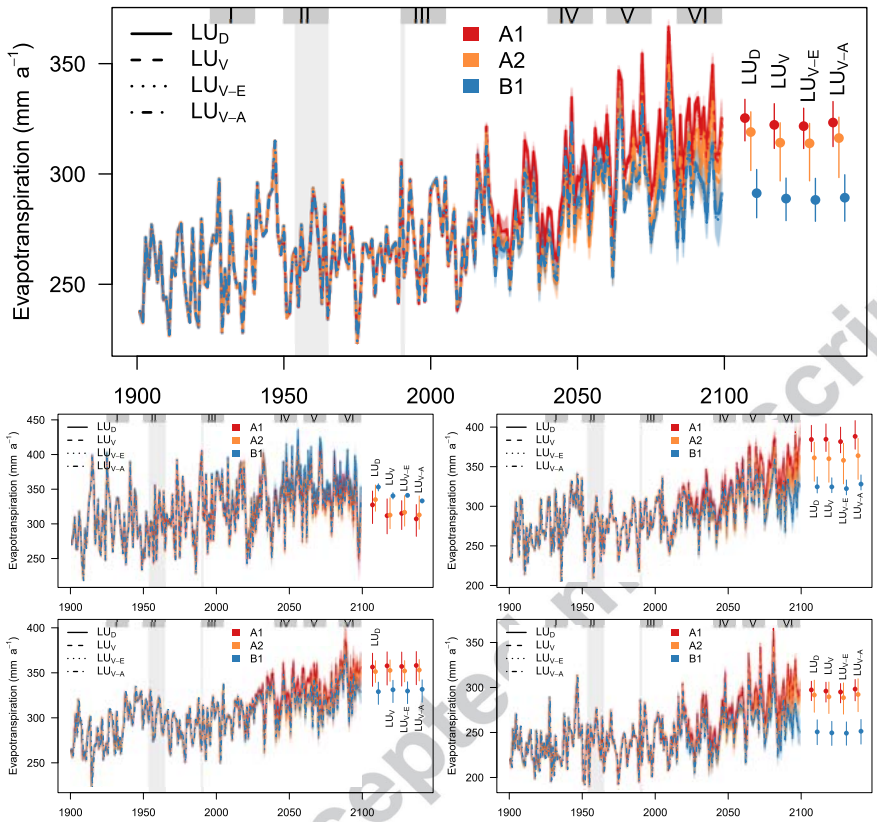

Fig. S10: Simulation results for annual evapotranspiration fluxes in the VLC region (mm a^{-1}) from 1900 to 2100 for the climate scenarios A1, A2 and B1 (color-coded; thick lines denote averages over three GMCs and shaded areas the range) and four different land-use data sets (line types). Shadings indicate VLC era and breakdown of the Soviet Union (light grey) and periods for further analysis (dark grey). Endpoints are denoted in right inset by dots (average values) and lines (ranges over three GCMs) per land-use dataset. The upper panel shows average values for the entire VLC region, and the lower figures for the four subregions R1 to R4.

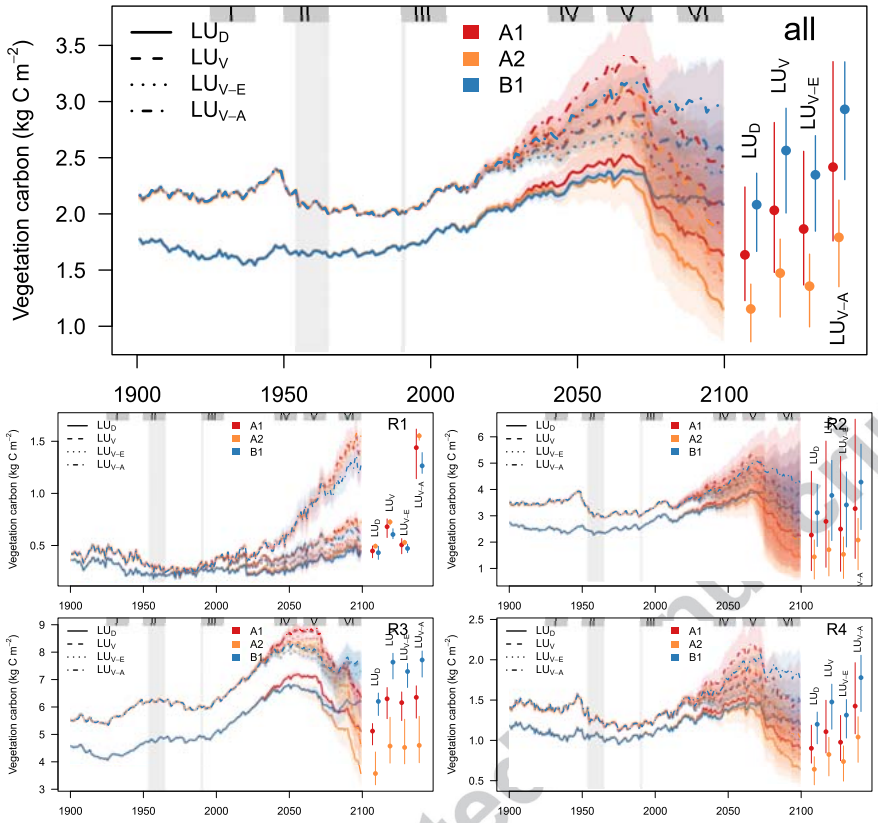

Fig. S11: Simulation results for vegetation carbon in the VLC region (kg C m^{-2}) from 1900 to 2100 for the climate scenarios A1, A2 and B1 (color-coded; thick lines denote averages over three GMCs and shaded areas the range) and four different land-use data sets (line types). Shadings indicate VLC era and breakdown of the Soviet Union (light grey) and periods for further analysis (dark grey). Endpoints are denoted in right inset by dots (average values) and lines (ranges over three GCMs) per land-use dataset. The upper panel shows average values for the entire VLC region, and the lower figures for the four subregions R1 to R4.

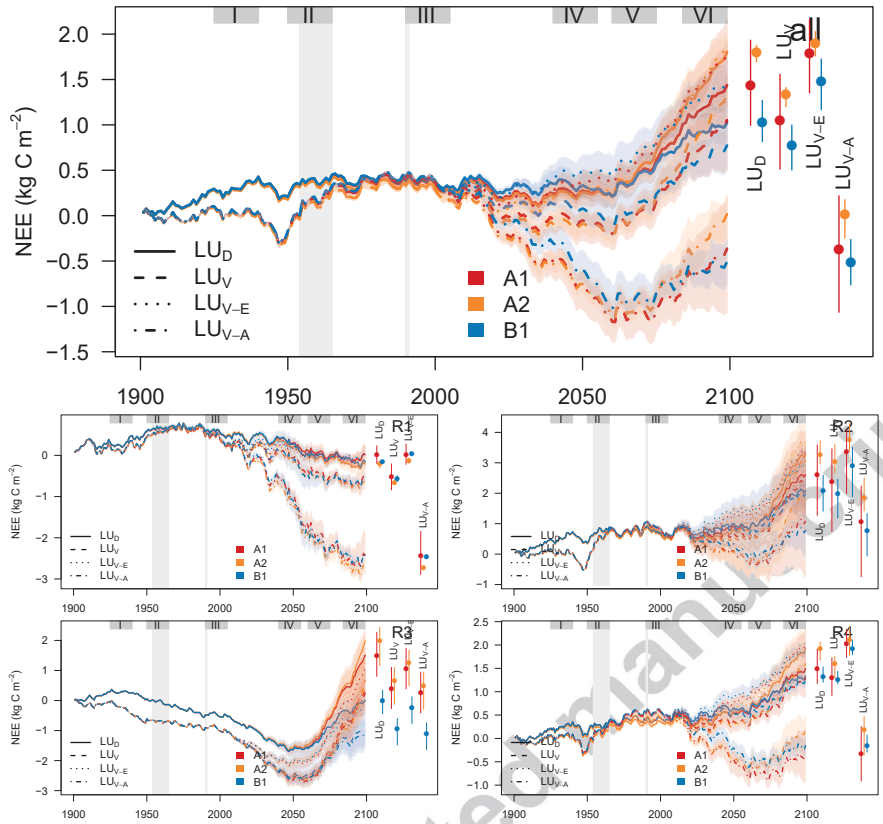

Fig. S12: Simulation results for cumulative carbon fluxes NEE in the VLC region (kg C m^{-2}) from 1900 to 2100 for the GLUES scenarios A1, A2 and B1 (color-coded; thick lines denote averages over three GMCs and shaded areas the range) and four different land-use data sets (line types). Shadings indicate VLC era and breakdown of the Soviet Union (light grey) and periods for further analysis (dark grey). Endpoints are denoted in right inset by dots (average values) and lines (ranges over three GCMs) per land-use dataset. The upper panel shows average values for the entire VLC region, and the lower figures for the four subregions R1 to R4. Negative values indicate a net carbon uptake by the land.